Met. Mater. Int., Vol. 24, No. 1 (2018), pp. 60~66
doi: 10.1007/s12540-017-7201-z

Metadynamic and Static Recrystallization Softening Behavior of a Bainite Steel

Lixin Li[1,3,*], Liangyu Zheng[3], Ben Ye[2,3], and Zeqiong Tong[3]

[1]The State Key Laboratory of Refractories and Metallurgy, Wuhan 430081, China
[2]Key Laboratory for Ferrous Metallurgy and Resources Utilization of Ministry of Education, Wuhan 430081, China
[3]Wuhan University of Science and Technology, Wuhan 430081, China

(received date: 18 March 2017 / accepted date: 19 July 2017)

The metadynamic recrystallization (MDRX) and static recrystallization (SRX) softening behavior of a bainite steel was investigated by two-pass isothermal compression experiments at temperatures of 1173, 1273, 1373, and 1473 K and strain rates of 0.01, 0.1, 1, and 10 s^{-1} with inter-pass times of 1, 5, 10, and 30 s on a Gleeble-1500 thermo-mechanical simulator. Kinetic equations were developed to evaluate the softening fractions caused by MDRX and SRX. A comparison between the experimental and predicted softening fractions showed that the proposed kinetic equations can provide a precise estimation of the MDRX and SRX behavior of the studied steel. The results based on the kinetic equations indicated that the MDRX and SRX softening fraction increases with the increase in strain rate, deformation temperature, inter-pass time, and pre-strain; the activation energy of MDRX is much smaller than that of SRX; and the no-recrystallization temperature of the investigated steel is 1179.4 K.

Keywords: alloys, hot working, recrystallization, compression test, kinetic equation

1. INTRODUCTION

Hot processes of alloys often need several successive deformation passes. In the inter-pass periods, either metadynamic recrystallization (MDRX) or static recrystallization (SRX), two softening mechanisms for alloys, will occur. Initiation and development of MDRX and SRX are very helpful to grain refinement and microstructural homogenization, which increase the subsequent mechanics and process performance of the products [1-4]. Therefore, it is necessary to investigate the critical conditions and softening behaviors of MDRX and SRX to design the most effective processing path and to optimize the deformation parameters for alloys.

When the stress and strain exceed their respective critical values for temperature and strain rate, dynamic recrystallization (DRX) will occur during the hot deformation, and MDRX will occur in the DRX microstructure during the inter-pass times [5,6]. When the critical conditions of DRX are not met, static recovery (SRV) or even SRX will occur during the subsequent insulation or cooling process [7]. Initiation of SRX depends on the temperature of alloys under certain deformation conditions. When the temperature is below a certain value, the no-recrystallization temperature, SRX will not occur. The no-recrystallization temperature is usually determined from the variation of mean flow stress with the inverse of deformation temperature. This determination process uses the average schedule, in which all deformation parameters are kept constant except temperature [8,9]. It is difficult to keep these parameters invariant. Therefore, it is necessary to investigate a new method of determining the no-recrystallization temperature for both theoretical research and industrial application.

The softening behavior of MDRX and SRX can be characterized by the Avrami equation, but essential differences exist. The former is affected by strain rate but not influenced by strain, while the latter is affected by strain but less influenced by strain rate [10]. Therefore, it is necessary to make a comparative study of the MDRX and SRX kinetics.

The alloy studied is a low carbon bainite steel used in construction machinery with moderate strength, superior plasticity and good weldability. Even though extensive work was carried out on the effect of composition and thermodynamic parameters on dynamic recovery, DRX, microstructure and mechanical properties [11-14], less attention has been paid to the MDRX and SRX critical conditions and softening behavior of this alloy. In this paper, the kinetic equations for the MDRX and SRX of the investigated steel were established. Effects of the deformation parameters on the MDRX and SRX softening behavior were analyzed, and a comparison of onset conditions and completion times for MDRX and SRX was made based on these equations.

*Corresponding author: lilixin@wust.edu.cn

2. EXPERIMENT PROCEDURE

2.1. Materials

The alloy studied is a Mn-Mo-B series bainite steel. Its chemical composition (wt%) is as follows: 0.053C-0.310Si-1.567Mn-0.014P-0.005S-0.246Mo-0.014Ti-0.236Ni-0.0012B. The steel was in the form of a 30 mm × 300 mm × 450 mm plate, which had been hot-rolled. Cylindrical specimens with a height of 15 mm and a diameter of 10 mm were machined from the hot-rolled plate. The axis of the specimen was selected in the direction of the plate thickness.

2.2. Method

Hot compression tests were conducted on a Gleeble-1500 thermo-mechanical simulator. Four different deformation temperatures of 1173, 1273, 1373, and 1473 K, strain rates of 0.01, 0.1, 1, and 10 s^{-1}, pre-strains or first-pass strains of 0.1, 0.2, 0.3, and 0.4 and inter-pass times of 1, 5, 10, and 30 s were used in the compression tests. To minimize friction and maintain the cylindrical shape of specimens during tests, graphite powder was put into two grooves with a diameter of 6 mm and a height of 0.2 mm, which were made on both ends of each specimen.

Specimens were first heated to 1473 K at a rate of 10 K/s, held isothermally for 5 min, then cooled to the deformation temperature at a rate of 3 K/s by a cooling gas of He and held isothermally for 2 min to eliminate thermal gradient before deformation. Samples were then compressed to the pre-strain, held isothermally for the preset inter-pass time, and finally compressed to $\varepsilon = 0.7$ (pre-strain and inter-pass time are zero for one-pass compression tests).

2.3. Results

True-stress-true-strain data were recorded by the testing system in an isothermal compression process. The results of a one-pass compression test are illustrated in Fig. 1(a), which shows the stress-strain relationship at a deformation temperature of 1273 K. The microstructure of a specimen deformed at 1273 K and 0.1 s^{-1} is shown in Fig. 1(b). There are three types of stress-strain curves: the first is characterized by the increase

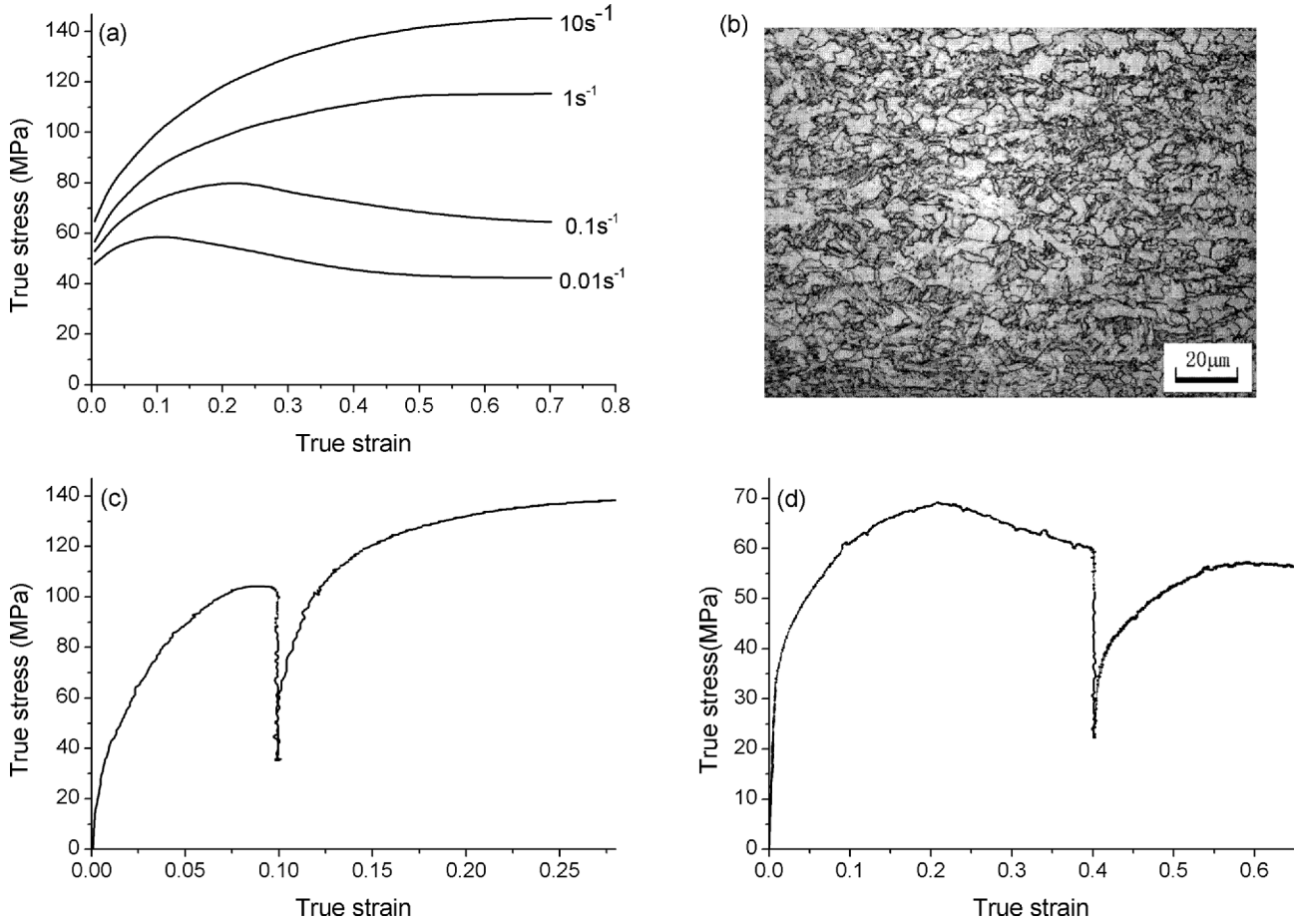

Fig. 1. Compression test results for the steel investigated; (a) the stress-strain curves at various strain rates at a temperature of 1273 K, (b) the microstructure of a specimen deformed at 1273 K and 0.1 s^{-1}, (c) the stress-strain curve of a two-pass compression test at a temperature of 1173 K, a stain rate of 1 s^{-1}, an inter-pass time of 30 s and a pre-strain of 0.1, and (d) the stress-strain curve of a two-pass compression test at a temperature of 1373 K, a stain rate of 0.1 s^{-1}, an inter-pass time of 5 s and a pre-strain of 0.4.

of flow stress with strain, which is demonstrated by the curve marked 10 s^{-1}; the second is characterized by a saturation stress with increasing strain, which is displayed in the curve labeled 1 s^{-1}; and the last is composed of three stages, hardening, softening and steady, which are shown in the curves marked 0.01 s^{-1} and 0.1 s^{-1}.

The stress-strain curve of a two-pass compression test at a deformation temperature of 1173 K, a strain rate of 1 s^{-1}, an inter-pass time of 30 s and a pre-strain of 0.1 is presented in Fig. 1(c). The figure shows that SRX occurs during the inter-pass time because the interruption is on the hardening stage of the stress-strain curve. The experimental results under a deformation temperature of 1373 K, a strain rate of 0.1 s^{-1}, inter-pass time of 5 s and a pre-strain of 0.4 are illustrated in Fig. 1(d). The figure shows that MDRX occurs during the inter-pass time because the interruption is on the softening stage of the stress-strain curve.

3. ANALYSIS

3.1. Calculation of MDRX and SRX softening fraction

The stress-strain curve is an external and comprehensive reflection of the microstructural evolution and deformation mechanisms [15]. Softening fractions caused by MDRX or SRX can be determined using the peak stress method, maximum stress method, offset-stress method, average stress method, and back-extrapolation method [16-19]. The offset-stress method, which is based on the relationship between stress variation and microstructure evolution during hot deformation, is widely used to calculate the softening fraction X. Therefore, the offset-stress method was utilized in this paper:

$$X = \frac{\sigma_m - \sigma_2}{\sigma_m - \sigma_1} \tag{1}$$

where σ_m is the flow stress corresponding to the first-pass unloading, and σ_1 and σ_2 are the yield stresses of the first pass and second pass, respectively.

The softening fraction calculated using the yield stresses at an offset strain of 0.2% is approximately the same as that determined from the average stress method [18]. The softening fraction is determined by the 0.2% offset method in this study.

3.2. Determination of MDRX and SRX experiment data

The relationship between the peak stress σ_p and the critical stress σ_c can be expressed by $\sigma_c/\sigma_p = 1.003155X^{-0.00016}$ and $\sigma_c = (0.997658 \pm 0.0008502)\sigma_p$ [20], where $Z = \dot{\varepsilon}\exp(Q/RT)$ is the temperature-compensated strain rate factor; thus, the condition required to reach critical stress for DRX is $1.003155Z^{-0.00016} \geq 0.9968078$, which can also be expressed as follows:

$$Z \leq 1.694 \times 10^{17} \tag{2}$$

The relation between peak strain ε_p and Z can be expressed by $\varepsilon_p = BZ$ [21]. A linear regression of the experimental data from the one-pass compression tests results in the material constants of $B = 9.72\times10^{-4}$ and $D = 0.1456$, meaning $\varepsilon_p = 0.92 \times 10^{-4}Z^{0.1456}$. Therefore, the condition for the alloy deformation to reach its critical strain ε_c of recrystallization can be expressed by Eq. (3), according to reference [20].

$$\varepsilon \geq 8.61642 \times 10^{-4} Z^{0.1456} \tag{3}$$

For MDRX to occur during the inter-pass time, DRX must also occur; therefore, Eqs. (2) and (3) describe a necessary condition for MDRX to occur. There are many crystal nuclei in the DRX areas. When the temperature is high enough, the crystal nuclei will continue to grow upward, namely occurrence of MDRX without the incubation period. Therefore, Eqs. (2) and (3) are sufficient condition for MDRX as well. Obviously, SRV or SRX will exist if Eqs. (2) and (3) are not satisfied.

3.3. Kinetic equation of MDRX

It is believed that the relationship between softening fraction X and time t can be described by the Avrami equation [22-24]:

$$X = 1 - \exp\left[-0.693\left(\frac{t}{t_{0.5}}\right)^n\right] \tag{4}$$

where n is the material constant, and $t_{0.5}$, the time for 50% recrystallization, can be expressed by Eq. (5) for MDRX [25,26].

$$t_{0.5}^m = A\dot{\varepsilon}^q \exp\left(\frac{Q_m}{RT}\right) \tag{5}$$

where A and q are material constants, and Q_m is the MDRX activation energy.

Equation (6) can be derived by combining Eqs. (4) and (5):

$$\ln[-\ln(1-X_m) + 0.366725] = n\ln A - nq\ln\dot{\varepsilon} - \frac{nQ_m}{RT} \tag{6}$$

where X_m is the softening fraction of MDRX.

The value of the material constants A, q, and n and activation energy Q_m can be determined by a linear regression of Eq. (6). It is easy to obtain the value of n at 1.542, and the time for 50% MDRX can be expressed as:

$$t_{0.5}^m = 1.625 \times 10^{-6}\dot{\varepsilon}^{-0.7538}\exp\frac{152157.6}{RT} \tag{7}$$

3.4. Kinetic equation of SRX

The relationship between the SRX softening fraction and the time for 50% recrystallization can be expressed by Eqs. (4) and (8) [27,28].

$$t_{0.5}^s = A\dot{\varepsilon}^p\varepsilon^q \exp\left(\frac{Q_s}{RT}\right) \tag{8}$$

where A, p, and q are the material constants, and Q_s is the SRX

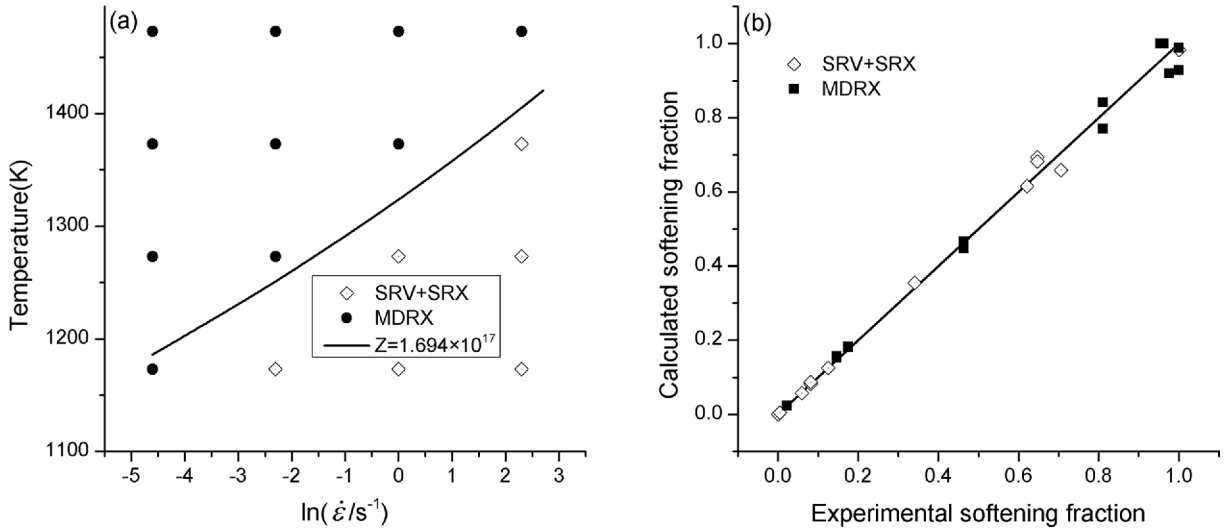

Fig. 2. Comparison between calculated and experimental DRX critical condition (a) and softening fraction (b).

activation energy.

The value of the material constants A, p, q, and n and activation energy Q_s can be determined by a linear regression of the experimental SRX data. The results show that n is equal to 0.9534, and the time for 50% SRX can be described by Eq. (9).

$$t_{0.5}^{s} = 7.0047 \times 10^{-14} \varepsilon^{-1.8925} \dot{\varepsilon}^{-0.5455} \exp\frac{320486.7}{RT} \quad (9)$$

3.5. Experimental verification

Whether DRX occurs during deformation can be determined by the stress-strain curve. It is widely accepted that the appearance of peak stress in the stress-strain curve is considered a sole and reliable signal of the initiation of DRX [29,30]. The results derived from the one-pass compression tests are shown in Fig. 2(a), which indicates that Eq. (2) can be used as a DRX criterion for the steel tested.

A comparison between the experimental and calculated softening fractions of MDRX and SRX is shown in Fig. 2(b). The results demonstrate that the relative errors of softening fraction are less than 7.4%. The intercept and slope of the regression line are -0.00727 and 1.00506, respectively, showing that most of the data points lie close to the best regression line. The correlation coefficient is 0.997311, indicating a good correlation between the experimental and calculated data. Therefore, the kinetic equations of (4), (7) and (4), (9) can satisfactorily describe the softening mechanisms of the MDRX and SRX of the investigated steel.

4. DISCUSSION

4.1. Influence of deformation parameters on softening fraction

The influence of the deformation parameters on the recrystallization softening fraction is shown in Fig. 3, in which the SRX softening fraction is calculated based on the critical strain of DRX. Obviously, the influence of strain rate, temperature, inter-pass time and pre-strain on the softening fraction is significant.

Variation of the softening fraction with strain rate is shown in Fig. 3(a). The softening fraction increases with the increase in strain rate because the greater the strain rate, the more serious the non-uniform deformation and lattice distortion within alloys. The reduced extent of dynamic recovery occurring at higher strain rates in turn produces a higher dislocation density [7,31]. The abovementioned effects increase the driving force of recrystallization and make the softening process easier.

The effects of temperature on the softening fraction are shown in Fig. 3(b). The softening fraction increases significantly with the increase in temperature. There are two reasons for this. First, the nucleation of recrystallization is a thermally activated process; thus, the higher the temperature is, the easier the formation of nuclei. Second, the diffusion of atoms speeds up, and dislocation movement and grain boundary migration becomes easier with the increase in temperature, which benefits grain growth [27,31].

The change of the softening fraction with inter-pass time is shown in Fig. 3(c). The softening fraction increases with the extension of inter-pass time because the recrystallized nuclei appear and grow to free-dislocation grains in the hot deformed structure through both dislocation climb and annihilation to contribute to alloy softening with increasing inter-pass time [17,27].

The effect of pre-strain on the SRX softening fraction is illustrated in Fig. 3(d), which shows that the softening fraction increases with the increase in pre-strain. This effect occurs because the increase of internal lattice distortion and dislocation density results in the increase in the recrystallization driving force with the increase in pre-strain [28].

Clearly, the SRX softening fractions involved in Fig. 3(a)-

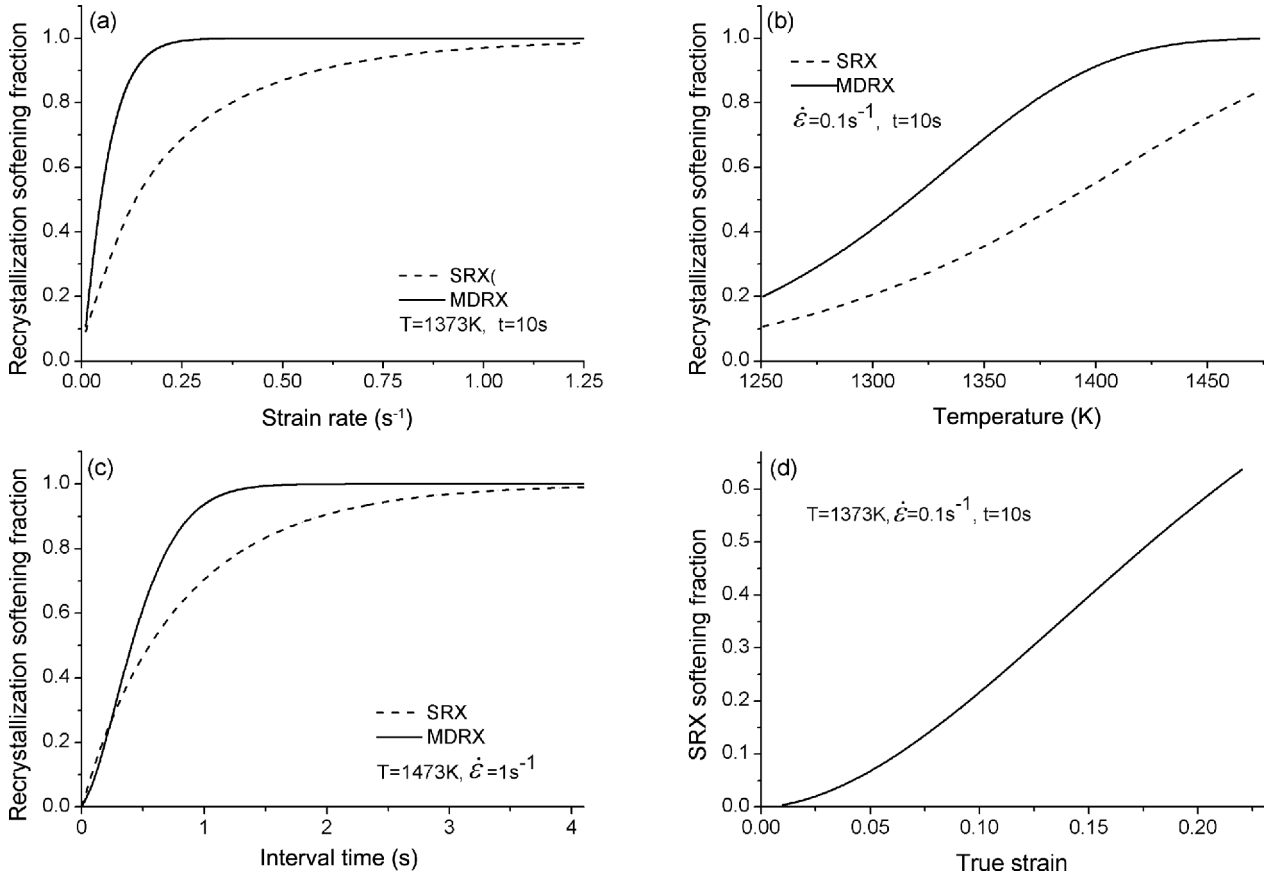

Fig. 3. Variations of recrystallization softening fraction with strain (a), temperature (b), interval time (c), and true strain (d).

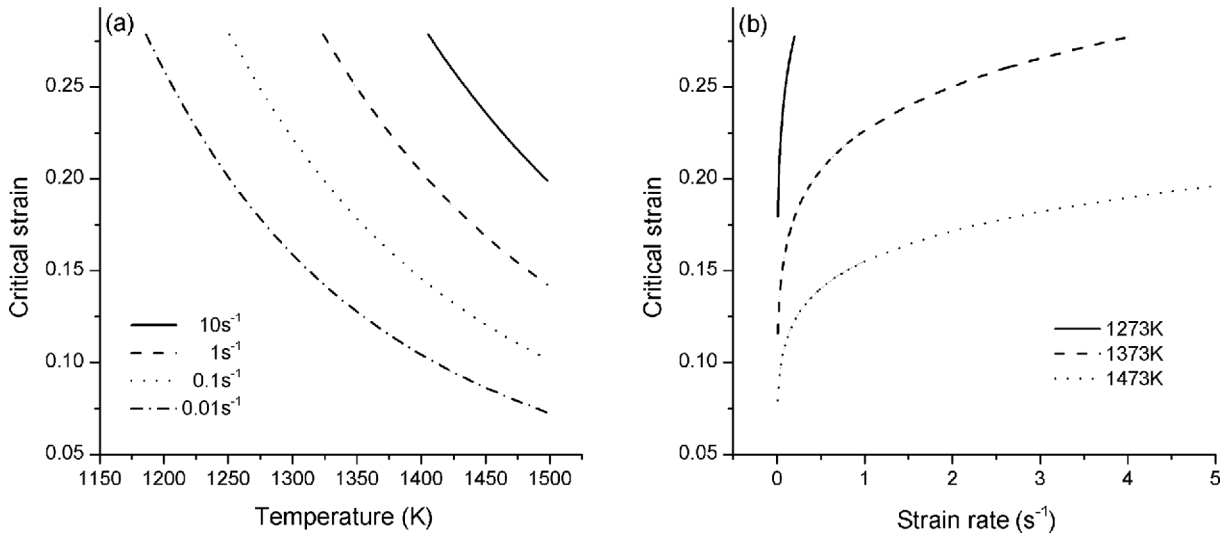

Fig. 4. Variations of critical strain with temperature (a) and strain rate (b).

3(c) are the maximum among all of the same strain rates, temperatures and inter-pass times. Further, it can be seen that the MDRX softening fractions are greater than the SRX fractions with the same deformation parameters, which suggests that MDRX is more likely to occur than SRX. This result is because the activation energy of MDRX is much smaller than that of SRX, as shown in Eqs. (7) and (9).

4.2. Condition for onset of MDRX and SRX

The critical condition of MDRX, or the relationship between

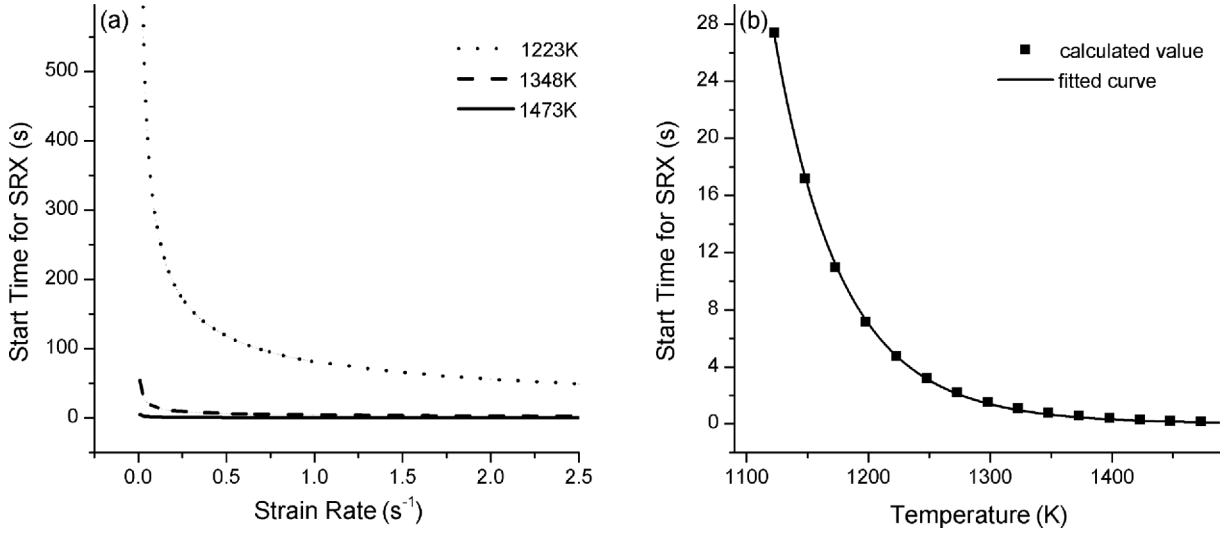

Fig. 5. Variations of start time for SRX with strain rate (a) and temperature (b).

the critical strain, deformation temperature, and strain rate described by Eqs. (2) and (3) is shown in Fig. 4. As indicated in Fig. 4(a), the critical strain and its reduction rate decrease with the increase in deformation temperature; the lower the strain rate is, the wider the temperature range of MDRX. However, it is very difficult for MDRX to occur even at a high deformation temperature when the strain rate is greater than a critical value. Another kind of expression of the MDRX condition is shown in Fig. 4(b), which indicates that the higher the deformation temperature is, the wider the strain rate range of MDRX occurrence; the critical strain increases rapidly with the decrease in deformation temperature; and it is impossible for MDRX to occur despite a lower strain rate when the deformation temperature is lower than a certain value.

The softening fraction calculated using the 0.2% offset method includes the softening effect of SRV. It is generally assumed that SRX starts when the softening fraction is equal to 0.2 [32,33], which means that $t^s_{0.2}$ is the start time for SRX. The relationship between $t^s_{0.2}$ and the deformation parameters is shown in Fig. 5(a), with a pre-strain of 0.1, which indicates that $t^s_{0.2}$ increases with the decrease in strain rate and temperature. There will exist only SRV, but no SRX, during the interpass times when the temperature is too low.

Clearly, it is appropriate to define the no-recrystallization temperature based on the variation of $t^s_{0.2}$ with temperature under given deformation conditions. Considering that the decrease of $t^s_{0.2}$ becomes weaker when the strain rate is larger than 1 s^{-1}, the temperature corresponding to $t^s_{0.2}$ of 10 s and the strain rate of 1 s^{-1} can be defined as the no-recrystallization temperature [8,34]. Obviously, when the temperature is higher than the no-recrystallization temperature, the softening behavior of austenite will occur over a period of 10 s. Furthermore, the no-recrystallization temperature is the lowest temperature corresponding to the critical strain of DRX. The relation between the temperature and $t^s_{0.2}$ is shown in Fig. 5(b), with solid points indicating when the critical strain and strain rate of 1 s^{-1} are adopted. It is easy to obtain the relation of $t^s_{0.2} = 3.98021 \times 10^{63} T^{-20.37974}$ and the no-recrystallization temperature of $T_{nr} = 1179.4$ K. This value is close to 1186 K for a Nb steel [35], but smaller than 1213 K and 1253 K for a Ti-V and Nb-V steel, respectively [8].

4.3. Completion time of MDRX and SRX

It is possible to determine the completion time of MDRX and SRX by the supposition that recrystallization stops at the point when the softening fraction is equal to 0.9 [36]. The variation in completion time for MDRX and SRX with temperature and strain rate is shown in Fig. 6, which indicates that MDRX is faster than SRX under conditions of the same temperature and strain rate, and the lower the temperature is, the

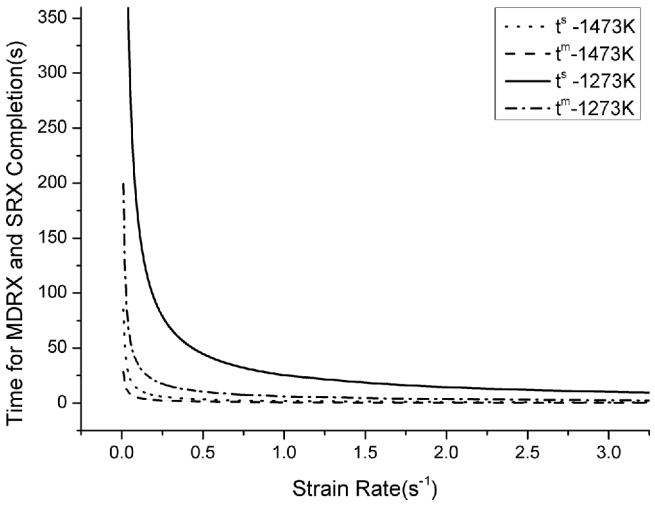

Fig. 6. Time for MDRX and SRX completion.

greater the difference; the effects of temperature and strain rate on completion time are significant when the strain rate is lower; and the effects of strain rate on completion time weaken when strain rate is more than 1 s^{-1}. The inter-pass time is usually 0.4-20 s, and the rolling temperature is lower than 1273 K for plate and strip finishing rolling [37]. Clearly, it is difficult to complete the MDRX and SRX during the inter-pass time for the steel investigated in this paper.

5. CONCLUSION

MDRX and SRX behaviors of a bainite steel were examined by two-pass isothermal compression experiments. The effects of deformation temperature, strain rate, pre-strain, and inter-pass time were studied in detail. The most important results can be summarized as follows.

(1) The MDRX and SRX kinetics equation of the alloy tested can be described by $X = 1-\exp[-0.693(t/t_{0.5})^n]$, of which the time for 50% recrystallization can be expressed as $t^m_{0.5} = 1.625 \times 10^{-6}\dot{\varepsilon}^{-0.7538}\exp(152157.6/RT)$ and $t^s_{0.5} = 7.0047 \times 10^{-14}\varepsilon^{-1.8925}\dot{\varepsilon}^{-0.5455}\exp(320486.7/RT)$, and n equals 1.542 and 0.9534, respectively.

(2) The necessary and sufficient conditions for MDRX are $\varepsilon \geq 8.6464 \times 10^{-4} Z^{0.1456}$ and $Z \leq 1.694 \times 10^{17}$. The no-recrystallization temperature of the alloy studied is $T_{nr} = 1179.4$ K.

(3) The softening fraction of MDRX and SRX increases with the increase in strain rate, deformation temperature, inter-pass time, and pre-strain.

REFERENCES

1. J. Liu, Y. G. Liu, H. Lin, and M. Q. Li, *Mat. Sci. Eng. A* **565**, 126 (2013).
2. Y. Cao and H. Di, *Mater. Lett.* **163**, 24 (2016).
3. F. Han, B. Tang, H. Kou, J. Li, and Y. Feng, *Prog. Nat. Sci. - Mater.* **25**, 58 (2015).
4. C. Zheng, N. Xiao, D. Li, and Y. Li, *Comp. Mater. Sci.* **44**, 507 (2008).
5. Y. Han, H. Wu, W. Zhang, D. Zou, G. Liu, and G. Qiao, *Mater. Design* **69**, 230 (2015).
6. Y. C. Lin, M. S. Chen, and J. Zhong, *J. Mater. Process. Tech.* **209**, 2477 (2009).
7. Y. C. Lin, M. S. Chen, and J. Zhong, *Comp. Mater. Sci.* **44**, 316 (2008).
8. L. N. Pussegoda and J. J. Jonas, *ISIJ Int.* **31**, 278 (1991).
9. A. I. Zaky, *J. Mater. Eng. Perform.* **15**, 651 (2006).
10. K. Arun Babu, S. Mandal, A. Kumar, C. N. Athreya, B. de Boer, and V. Subramanya Sarma, *Mat. Sci. Eng. A* **664**, 177 (2016).
11. F. Chen, Z. Cui, D. Sui, and B. Fu, *Mat. Sci. Eng. A* **540**, 46 (2012).
12. W. F. Cui, S. X. Zhang, Y. Jiang, J. Dong, and C. M. Liu, *Mat. Sci. Eng. A* **528**, 6401 (2011).
13. H. K. Sung, D. H. Lee, S. Y. Shin, S. Lee, J. Y. Yoo, and Y. Hwang, *Mat. Sci. Eng. A* **624**, 14 (2015).
14. X. Kong, L. Lan, Z. Hu, B. Li, and T. Sui, *J. Mater. Process. Tech.* **217**, 202 (2015).
15. M. A. Mostafaei and M. Kazeminezhad, *Mat. Sci. Eng. A* 544, 88 (2012).
16. L. Li, B. Ye, S. Liu, S. Hu, and B. Li, *Mat. Sci. Eng. A* **636**, 243 (2015).
17. Y. C. Lin, L.-T. Li, and Y.-C. Xia, *Comp. Mater. Sci.* **50**, 2038 (2011).
18. Y. C. Lin, X.-M. Chen, M.-S. Chen, Y. Zhou, D.-X. Wen, and D.-G. He, *Appl. Phys. A* **122**, 601 (2016).
19. G. Li, T. M. Maccagno, D. Q. Bai, and J. J. Jonas, *ISIJ Int.* **36**, 1479 (1996).
20. L. Li, B. Ye, S. Liu, S. Hu, and H. Liao, *J. Mater. Eng. Perform.* **25**, 4581 (2016).
21. Y. C. Lin, X. Fang, and Y. P. Wang, *J. Mater. Sci.* **43**, 5508 (2008).
22. M.-S. Chen, Y. C. Lin, and X.-S. Ma, *Mat. Sci. Eng. A* **556**, 260 (2012).
23. F. Jiang, H. Zhang, L. Li, and J. Chen, *Mat. Sci. Eng. A* **552**, 269 (2012).
24. A. Paggi, G. Angella, and R. Donnini, *Mater. Charact.* **107**, 174 (2015).
25. H. Wu, L. Du, Z. Ai, and X. Liu, *J. Mater. Process. Tech.* **29**, 1197 (2013).
26. H. Jiang, L. Yang, J. Dong, M. Zhang, and Z. Yao, *Mater. Design* **104**, 162 (2016).
27. S. H. Cho, K. B. Kang, and J. J. Jonas, *Mater. Sci. Tech.* **18**, 389 (2002).
28. Y. G. Liu, J. Liu, M. Q. Li, and H. Lin, *Comp. Mater. Sci.* **84**, 115 (2014).
29. M. Jin, B. Lu, X.-G. Liu, H. Guo, H.-P. Ji, and B.-F. Guo, *J. Iron Steel Res. Int.* **20**, 67 (2013).
30. I. Mejia, A. Bedolla-Jacuinde, C. Maldonado, and J. M. Cabrera, *Mat. Sci. Eng. A* **528**, 4133 (2011).
31. R. Ding and Z. X. Guo, *Acta Mater.* **49**, 3163 (2001).
32. D.-Q. Dong, F. Chen, and Z.-S. Cui, *J. Iron Steel Res. Int.* **23**, 466 (2016).
33. W. P. Sun and E. B. Hawbolt, *ISIJ Int.* **37**, 1000 (1997).
34. X.-M. Hu, Q. Gao, B.-C. Zhao, F.-H. Liang, C. Wang, and L.-G. Ao, *Heat Treat. Met.* **36**, 18 (2011).
35. S. Yue, D. Q. Bai, and J. J. Jonas, *Can. Metall. Quart.* **33**,145 (1994).
36. F. H. Samuel, S. Yue, J. J. Jonas, and B. A. Zbinden, *ISIJ Int.* **29**, 878 (1989).
37. R.-Z. Wang, Z.-M. Yang, and Y.-M. Che, *J. Iron. Steel Res.* **18**, 33(2006).